Gulf Stream–Generated Topographic Rossby Waves

ROBERT S. PICKART

Woods Hole Oceanographic Institution, Woods Hole, Massachusetts

(Manuscript received 11 October 1993, in final form 13 June 1994)

ABSTRACT

An inverse ray tracing model is applied to observations of 40-day topographic Rossby waves on the continental slope off of Cape Hatteras, North Carolina, to determine their origin. The rays are traced seaward and extend into the deep Gulf Stream, where the bottom slope remains strong enough that topographic β dominates planetary β. This enables coupling to occur between eastward propagating Gulf Stream meanders and topographic waves with eastward phase speed and matching zonal wavelength. Previous satellite observations indicate that the most frequently occurring Gulf Stream meanders have a period of 40 days, and the model reveals that, as these meanders pass a topographic bend near 71°–72°W, they are able to couple to the observed topographic waves traced back from Cape Hatteras. The 40-day Gulf Stream meanders occur in bursts, which leads to associated bursts of the topographic waves.

1. Introduction

Previous moored arrays along the continental slope of the Mid-Atlantic Bight have revealed that the deep mesoscale variability is dominated by topographic Rossby waves (e.g., Thompson and Luyten 1976; Johns and Watts 1986). In general, the observed dispersion characteristics of the waves agree nicely with topographic wave theory (e.g., Pickart and Watts 1990). The waves exist at periods from roughly 10 days—which is the theoretical high frequency cutoff (Johns and Watts 1986)—to 60 days. At longer periods the wave energy dies out (e.g., Welsh et al. 1991; Schultz 1987).

The source of the waves is believed to be the deep Gulf Stream, which flows relatively close to the boundary in the Mid-Atlantic Bight (Fig. 1). The observed phase propagation of the waves is offshore while the energy propagation is onshore, consistent with such an offshore source. Of course, as the Gulf Stream separates near Cape Hatteras, it flows directly over the continental slope, although it does not extend to the bottom here (Fig. 1). In this region the observed deep topographic waves are decoupled from the local surface meanders of the current (Johns and Watts 1986; Pickart and Watts 1990). This suggests as well that the waves are forced elsewhere—possibly further downstream where the Gulf Stream deepens—then propagate into the region (Fig. 1).

While the deep Gulf Stream is implicated as the obvious source of the topographic waves, the precise generation mechanism(s) is still unclear.[1] Several different mechanisms have been investigated. Louis et al. (1982) presented evidence that bursts of topographic waves observed off of Nova Scotia are associated with the formation of warm Gulf Stream eddies. The barotropic model by Louis and Smith (1982) of an eddy over a slope produced radiative solutions consistent with the observations. Hogg (1981) suggested that the topographic waves measured south of Cape Cod during the RISE experiment might be the result of one particularly large, prolonged Gulf Stream meander. Schultz (1987) also suggested that a burst of wave energy on the continental slope northeast of Cape Hatteras might be linked with a series of large amplitude Gulf Stream meanders further offshore. These latter two suggestions, while compelling, were nonetheless speculative.

It is difficult to imagine that the persistent wave energy observed in the Mid-Atlantic Bight is due completely to sporadic Gulf Stream events such as eddy formation or abnormally large path convolutions. The more common propagating meanders of the Gulf Stream might be considered as a (more continual) source. However, simple theory suggests that this would not be the case. As detailed by Pedlosky (1977), in order for propagating meanders to radiate energy they must have westward phase speed (to match that of the Rossby waves). Gulf Stream meanders are predominantly eastward, for which only trapped solutions are possible. More recent studies have demonstrated,

Corresponding author address: Dr. Robert S. Pickart, Woods Hole Oceanographic Institution, Department of Physical Oceanography, Woods Hole, MA 02543.

[1] It should be remembered that the Rossby waves observed on the continental slope are not necessarily topographic Rossby waves at their point of origin offshore; a planetary Rossby wave over a flat bottom that impinges onto a slope will become a topographic wave as topographic β dominates planetary β.

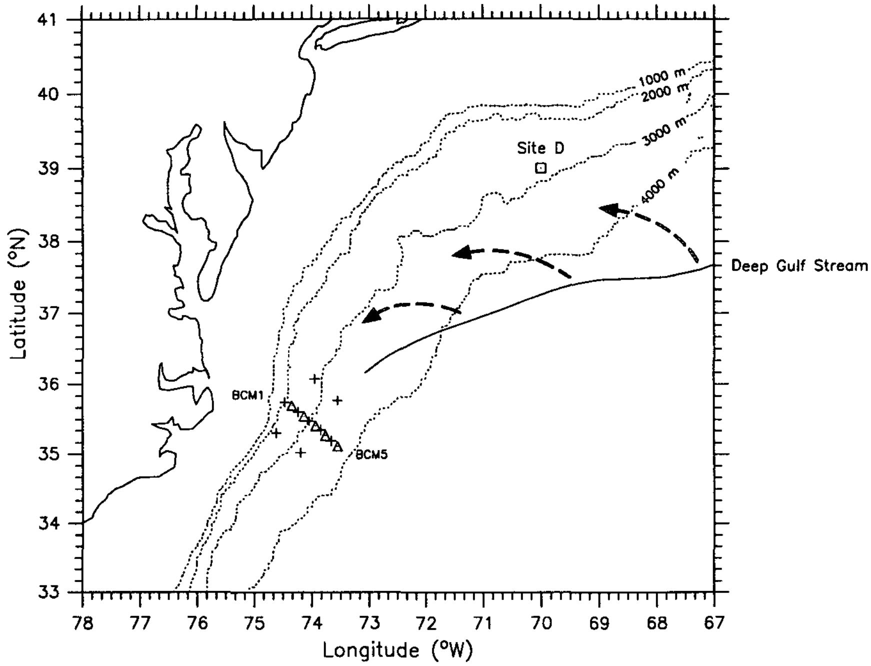

FIG. 1. SYNOP Inlet array maintained from October 1987 to September 1990; △: near bottom current meter (100 m above the bottom), +: Inverted Echo Sounder. The current meters are labeled BCM1 to BCM5 (onshore to offshore). The solid line is the mean axis of the deep Gulf Stream (which first reaches the bottom near 73°W). This was calculated using the mean north wall (from Olson et al. 1983; P. Cornillon 1992, personal communication) in conjunction with moored velocity data (from Halkin et al. 1985; Johns et al. 1994). The large dashed lines are a schematic representation of topographic Rossby waves emanating from the deep Gulf Stream and refracting as they encounter the increased bottom slope onshore (see Bower and Hogg 1992). Also shown is the Site D location where topographic waves have been previously observed (Thompson and Luyten 1976).

however, that in certain cases eastward propagating meanders can radiate energy. Hogg (1988) showed that energy radiation occurs if the meanders are modulated in space and time, that is, if the meander amplitude varies alongstream and if it has a growth-decay lifetime. This result is intriguing in light of the RISE observations. Rizzoli et al. (1994) suggested that in the presence of a significant bottom slope, coupling can occur between eastward propagating Gulf Stream meanders and radiating waves.

Rizzoli et al.'s (1994) idea is as follows. In regions where the Gulf Stream flows over nearly flat topography the meanders must couple to planetary Rossby waves; and since the waves have westward phase speed, such coupling is not possible (as explained above). However, if the Gulf Stream flows over a large enough bottom slope then coupling can occur with topographic Rossby waves. Because the strong topography aligns the Rossby wave dispersion curve along the bathymetry, if the isobaths are oriented with a nonzero meridional component this allows waves with an eastward component of phase speed (Fig. 2). In Rizzoli et al.'s (1994) model the Gulf Stream flowed over strong bottom slope near (the idealized representation of) Cape Hatteras and the Grand Banks; these two regions were characterized by enhanced radiative energy from the Gulf Stream, presumably by this coupling.

This paper presents results from a three-year deployment of bottom current meters at Cape Hatteras which reveal a strikingly pronounced topographic wave signal. An inverse wave tracing model is implemented to determine where the waves originate and to establish the wave characteristics offshore. The model, in conjunction with the moored data and additional Gulf Stream SST data, demonstrates convincingly that the waves are generated via the mechanism of Rizzoli et al. (1994) by eastward propagating Gulf Stream meanders. Furthermore, the meanders that generate the waves occur in regular bursts, leading to associated bursts of the topographic waves.

2. The topographic wave field

The Inlet array of the Synoptic Ocean Prediction experiment (SYNOP) was maintained off of Cape Hatteras, North Carolina, from fall 1987 to fall 1990, just shy of three years. It contained a single line of near-bottom current meters situated across the ther-

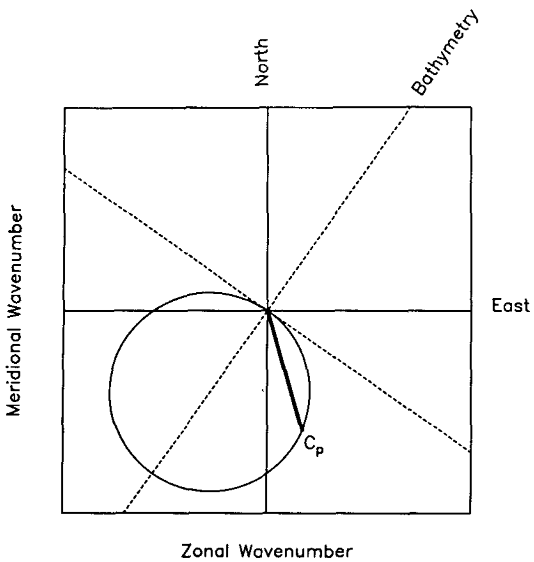

FIG. 2. Schematic of the barotropic topographic Rossby wave dispersion curve for bathymetry oriented southwest to northeast as in Fig. 1 (after Rizzoli et al. 1994). This allows for waves with an eastward component of phase speed (C_p) as shown.

mohaline deep western boundary current (DWBC) surrounded by an array of Inverted Echo Sounders (IESs), which simultaneously measured the thermocline topography of the upper-layer Gulf Stream. This location is where the separating Gulf Stream crosses over the equatorward flowing DWBC (Fig. 1). For details of the array the reader should consult Pickart et al. (1992a).

Pickart and Watts (1990) analyzed the first 8 months of data from this array and described the topographic waves. The deep velocity records were dominated by a particularly energetic wave signal at a period of roughly 40 days. Pickart and Watts (1990) showed that the orientation of the wavevector deduced from the observations agreed well with that predicted from linear topographic wave theory. The authors were puzzled, however, as to why such a pronounced signal should exist at 40 days, and they wondered whether or not it would persist.

Indeed, the full 3-year records reveal a pronounced spectral peak near 40 days (Fig. 3), demonstrating the persistence of this signal. The full dataset also allows us to determine the longer timescale modulation of the wave field, that is, how the amplitude of the 40-day wave varies in time. The method of complex demodulation was used (e.g., see Rosenfeld 1987). In particular, the 3-year record of alongslope velocity was bandpassed, permitting the signal between 10–80 days. Then, individual 120-day segments of the time series were fit via least squares to a 40-day sine wave, $A \sin(\omega t + \phi)$, where successive segments were shifted by 20 days over the length of the record. The resulting time series of A (the wave amplitude) reveals that the 40-day waves occur in bursts, where the average duration of each burst is 230 days (Fig. 4). It should be noted that these peaks are significant at the 95% confidence level. Interestingly, the bursts have an alternating character: every other burst is felt at all locations across the slope, whereas the bursts in between are present only at the offshoremost site (Fig. 4). This notion is supported by the observed time variation in correlation of velocity between the different sites. For example, consider the first two bursts in Fig. 4 (the bursts are delimited by the dashed lines). During the first burst the alongslope flow at sites BCM5 and BCM2 is strongly

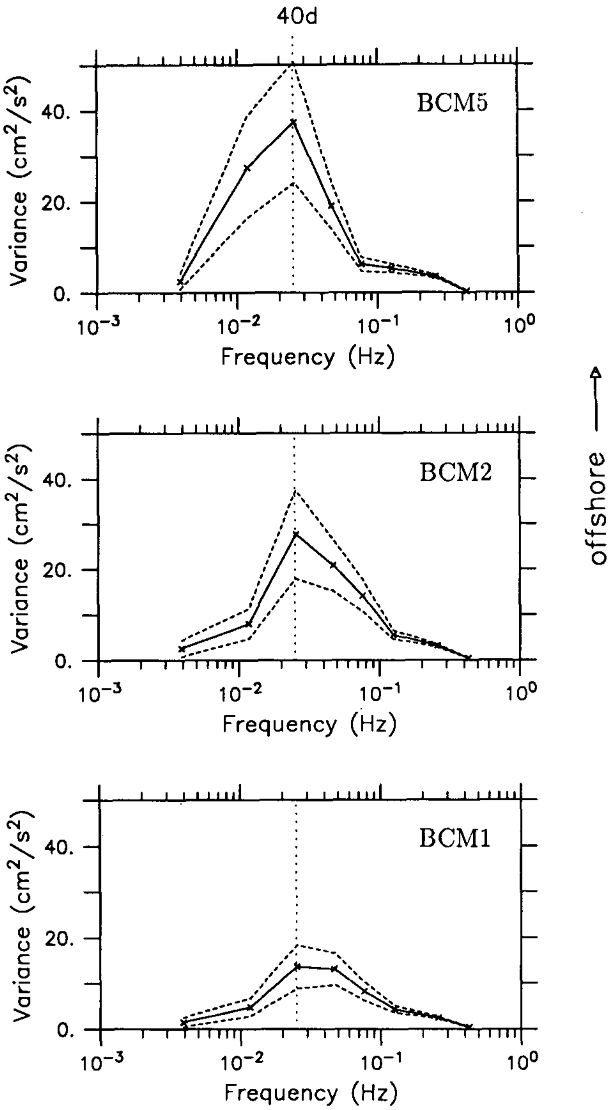

FIG. 3. Variance-preserving autospectrum of alongslope current from the bottom current meters. Only three of the instruments (BCM1, BCM2, BCM5; Fig. 1) had continuous three-year records, all showing a pronounced peak near 40 days. The dashed lines are the 95% confidence limits indicating that in each case the peak is significant.

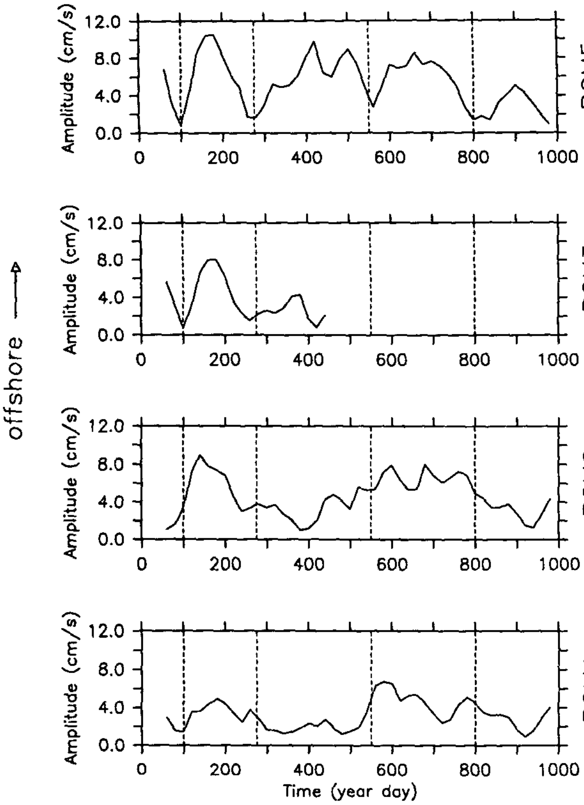

FIG. 4. Amplitude of the 40-day signal in alongslope current (from complex demodulation) at the different instrument sites, where year day 1 corresponds to 14 October 1987. The dashed lines delimit the four bursts occurring at the offshoremost site.

coherent at 40 days (with 95% confidence) with the expected offshore phase lag (see Pickart and Watts 1990). This is in marked contrast to the second burst for which there is no such correlation. The regularity of these bursts suggests a periodic nature to the forcing (as opposed to random sporadic events). In an effort to determine the source of the wave bursts, a ray-tracing model was developed.

3. Inverse ray tracing model

Following the ideas in Hogg (1981), a numerical model was developed to trace the ray paths of the topographic waves from their point of observation at the Inlet array back into the basin interior; this would determine the character of the waves offshore and presumably help determine their source. The details of model are described in Meinen et al. (1993).

a. Dynamics

The governing equation for the Rossby waves is the linear quasigeostrophic potential vorticity equation

$$\frac{\partial}{\partial t}\left[p_{xx} + p_{yy} + \left(\frac{f_0}{N}\right)^2 p_{zz}\right] + \beta p_x = 0, \qquad (1)$$

where x and y are east and north, z is positive upwards, p is pressure, $f = f_0 + \beta y$ is the coriolis parameter, and N is the (constant) Brunt–Väisälä frequency. The associated boundary conditions are a rigid lid and no normal flow through the bottom,

$$\frac{\partial}{\partial t} p_z = 0 \quad \text{at} \quad z = 0, \qquad (2)$$

$$\frac{\partial}{\partial t} p_z = \frac{N^2}{f_0}(p_x h_y - p_y h_x) \quad \text{at} \quad z = -h. \qquad (3)$$

Substituting a solution of the form

$$p = A(z)e^{i(kx+ly-wt)} \qquad (4)$$

into (1) and using the boundary conditions (2) and (3) results in a coupled set of algebraic equations, which together comprise the dispersion relation

$$\lambda_v^2 = \left(k^2 + l^2 + \frac{\beta k}{\omega}\right)\left(\frac{N}{f_0}\right)^2, \qquad (5)$$

$$\lambda_v \tanh(\lambda_v h) = \frac{N^2}{\omega f_0}(kh_y - lh_x), \qquad (6)$$

where $1/\lambda_v$ is the vertical trapping scale of the wave.

In regions of strongly sloped topography such that planetary β can be ignored, and in the large stratification/short wave limit, these equations simplify to the more familiar dispersion relation considered in Johns and Watts (1986) and Pickart and Watts (1990) (these authors also used a rotated coordinate system aligned with the topography). While these are valid assumptions on the steep part of the continental slope, the present interest is to consider changes in the waves between this region and the more gently sloped topography further offshore. Thus, the coupled set (5) and (6) must be used.

As in Hogg (1981), the WKB limit is considered, where changes in the wave amplitude and phase due to the environment are assumed to vary on scales larger than the local wavelength. Admittedly the model will stretch this assumption; however, as explained below, the environmental parameters have been smoothed to remove the small scales of variability, and in fact the model wavelengths remain reasonably small in the WKB sense. It should be remembered that the WKB assumption often works beyond its formal limit and has been successfully applied under conditions much more extreme than those considered here (e.g., Bower and Hogg 1992).

Under the WKB approximation the equations governing the path of the wave and its wavenumber are (see LeBlond and Mysak 1978)

$$\frac{D\mathbf{x}}{Dt} = \frac{\partial\omega}{\partial\mathbf{k}} = \mathbf{c}_g, \qquad (7)$$

$$\frac{D\mathbf{k}}{Dt} = \sum_{i=1}^{n} -\frac{\partial\omega}{\partial\gamma_i}\nabla\gamma_i, \qquad (8)$$

where

$$\frac{D}{Dt} = \frac{\partial}{\partial t} + \mathbf{c}_g \cdot \nabla$$

is the derivative following the wavegroup, $\mathbf{x}$ is the location of the wavegroup (i.e., the ray), $\mathbf{k} = (k, l)$ is the wavenumber, and $\mathbf{c}_g$ is the group velocity. The γ_i are the environmental parameters that cause refraction of the wave. In this case there are three such parameters: h (water depth), ∇h (bottom slope), and N (Brunt–Väisälä frequency).

b. Model representation

An important feature of the model is that it contains realistic descriptions of the environmental parameters. For the bathymetry, the DBDB5 (5 n mi resolution) digitized bathymetry of the North Atlantic was used. After the area of interest was chosen (the Mid-Atlantic Bight), all the seamounts were removed from the dataset because of their large aspect ratio. The bathymetry was then smoothed using a filter width of 150 km, otherwise rays might respond to small-scale undulations in the bottom in violation of the WKB approximation. The inshore boundary of the model was taken to be the 2500-m isobath because farther onshore the smoothing results in unrealistic topography (due to the large gradient of the upper slope). This does not cause a problem because the data indicate that the wave energy is drastically reduced inshore of 2500 m (Pickart and Watts 1990). The final step was to fit a two-dimensional spline to the smoothed bathymetry, which readily enables computation of h and ∇h at any location in the domain. The spline representation is compared to the original DBDB5 data in Fig. 5, which shows that it is indeed an accurate low pass. The model bathymetry was also compared to high-resolution sonic bathymetry obtained in the region of the Inlet array (Pickart et al. 1992b), and the model continental slope compared quite favorably to the in situ data (again a realistic low pass).

To describe a topographic Rossby wave it is necessary to know the buoyancy frequency N. For the bottom-trapped waves on the continental slope one typically uses a representative subthermocline value, and this has led to favorable agreement between observed and predicted trapping scales (e.g., Johns and Watts 1986). In the model it was assumed that N was a function of bottom depth h, the rationale being that as a wave progresses up the continental slope it should experience a larger subthermocline N. To quantify this, historical CTD data from ten sections across the continental slope were used to compute the average value of N over the bottom 1000 m. A clear trend versus bottom depth was found, with roughly a 50% increase in subthermocline N from $h = 4500$ m to $h = 2500$ m. This trend was fit by a spline (Fig. 6) and included in the model, although model solutions were sensitive only at the 10% level to such variation.

c. Results

The model was applied as follows. At the site of the Inlet array the period (40 days) and wavelength (130 km) of the topographic waves were calculated from the data. The wavelength is given by $\lambda = (360/\bar{\phi})\overline{\Delta s} \times \cos(\Delta\theta)$, where $\bar{\phi}$ is the average phase offset of the wave between instrument sites, $\overline{\Delta s}$ is the average instrument spacing, and $\Delta\theta$ is the relative angle between the mooring line and wave vector. [The direction of the wave vector is determined by the principle axis variance ellipses; see Pickart and Watts (1990).] The associated group velocity was then determined using the bathymetry and stratification. These variables were put into the model as initial conditions. The model was then run in inverse mode (i.e., with a negative time step) using Eqs. (7) and (8) to compute the previous location and wavenumber of the wave. The group velocity was then recomputed and the process iterated. In this manner a ray was traced out and the changing features of the wave documented.

The rays emanating from the Inlet array mooring sites reveal the strong refraction that occurs due to the increased bottom slope onshore (Fig. 7). Farther offshore (nearer to its source) the wavelength increases (Fig. 8a), as does the vertical trapping scale (Fig. 8b). Clearly, it is the bottom slope ∇h which has the greatest effect on the wave characteristics. This can be seen by plotting the local bottom slope following the wave (Fig. 8d), which mirrors the wavelength and trapping scale trends, that is, weak bottom slope results in large wavelengths and large trapping scales. This is in contrast to the other environmental parameters h (Fig. 8b) and N (Fig. 8e) that do not as strongly reflect the wave trends, although they do have an effect. For example, the increase in h down the slope results in the overall decrease in group velocity (Fig. 8c).

Thus, at the Inlet site where the waves are observed, they are bottom trapped (vertical scale < bottom depth) and in the short wave limit—consistent with the other observations of topographic waves on the continental slope of the Mid-Atlantic Bight. Farther offshore, however, they become barotropic (Fig. 8b). Also, for a large distance offshore topographic β continues to dominate planetary β (Fig. 8f), even as the bottom slope decreases substantially. Thus, the model reveals that away from the Inlet array the waves become nearly barotropic topographic Rossby waves.[2]

[2] To be strictly barotropic the trapping scale must be much greater than the water depth, which does not happen until east of 68°W (Fig. 8b); however, away from the steepest part of the continental slope the trapping scale approaches the water depth.

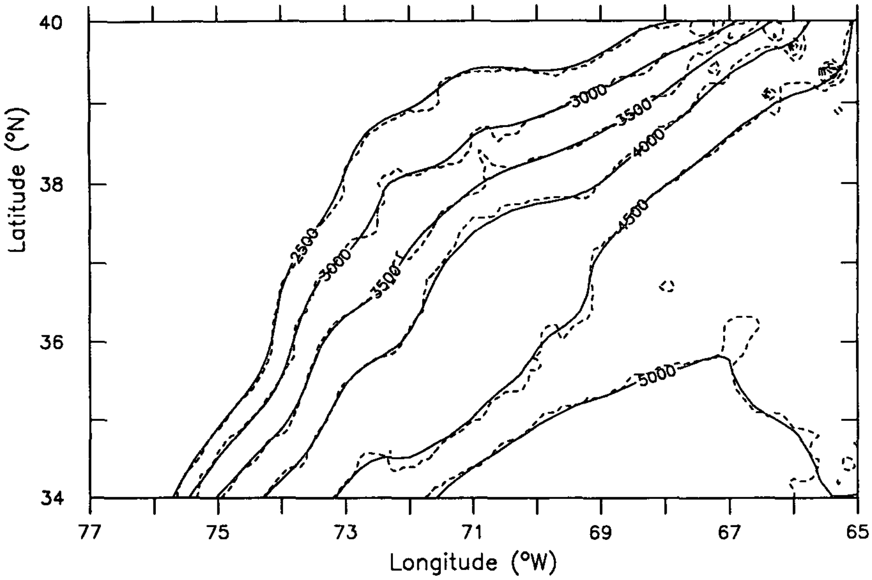

FIG. 5. Spline representation of the smoothed bathymetry (solid lines) used in the model, compared to the raw DBDB5 digitized bathymetry (dashed lines).

4. Generation mechanism

a. Meander–wave coupling

That the 40-day Rossby waves remain topographic away from the Inlet array into the region of the deep Gulf Stream (Fig. 7) suggests that the mechanism of Rizzoli et al. (1994) might be responsible for their generation, that is, coupling of the eastward propagating meanders of the Gulf Stream to the topographic waves. The increased vertical scale of the waves in this region would make the coupling more efficient. In fact, there is strong evidence that such coupling occurs.

An analysis of the Gulf Stream SST front between 74° and 60°W using 8 years of data (Lee 1994) indicates that the most frequently occurring meander in the Gulf Stream has a wavelength of 370 km and phase speed of 9 km d^{-1} to the east, which corresponds to a period of 40 days—precisely the spectral peak of the topographic waves in the Inlet array. In order for the coupling to occur, the topographic waves need to have an eastward component of phase speed and a zonal wavelength equal to the Gulf Stream meander wavelength. Figure 8g plots the zonal wavelength of the wave from the model, and indeed there is a region, from 71° to 72°W (indicated by shading), where the wavelength approximately matches that of the 40-day Gulf Stream meanders (note: a perfect match could be obtained by slightly altering the starting wavelength at the Inlet array). Close inspection of the bathymetry shows that in the region near 71°–72°W at the latitude of the Gulf Stream there is a northward bend in the bathymetry (shaded region, Fig. 9a). This increased northerly orientation is, in fact, needed to tilt the Rossby wave dispersion relation enough to cause a significant component of eastward phase propagation and hence the coupling.

To demonstrate this, the dispersion curve (l vs k at the 40-day period) was calculated at four locations along the Gulf Stream indicated by the numbers 1–4 in Figure 9a. The locations were chosen to correspond to different regions of isobath orientation. Note that the bathymetry has the largest northward orientation at location 2. The dispersion curve at each of the numbered sites is shown in Fig. 9b as the heavy solid curve, where the along- and cross-isobath directions are indicated by the small dashed lines. At site 2, the dis-

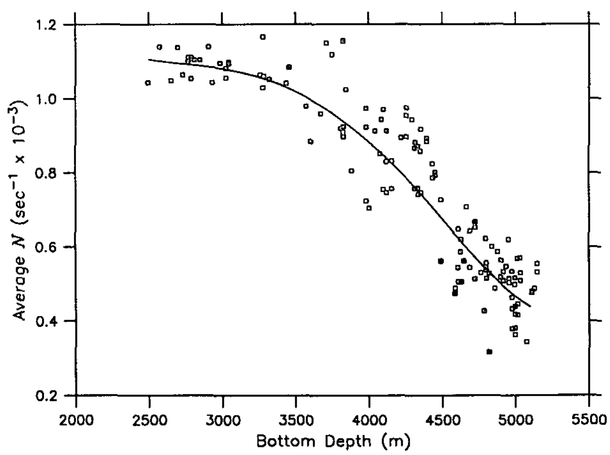

FIG. 6. Variation of Brunt–Väisälä frequency used in the model (solid line), which is a spline fit to the collection of historical stations (discrete points) as discussed in the text.

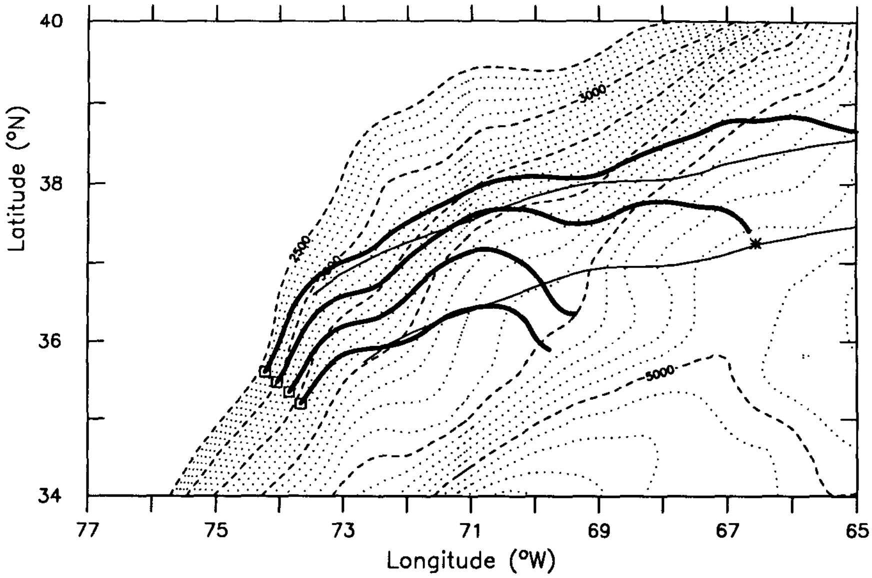

FIG. 7. Ray paths of the 40-day Rossby waves (dark lines) traced backwards from locations across the Inlet line. The thin solid lines denote the mean footprint of the deep Gulf Stream (which first reaches the bottom near 73°W, see caption to Fig. 1). The asterisk denotes the ray for which the features are described in Fig. 8.

persion curve has the greatest eastward extent leading to more easterly phase speeds. There are two reasons for this. The first is due to the northward orientation of the bathymetry as pointed out. Note, however, that at location 4 (which also has significant northward topographic orientation) the dispersion curve veers more sharply away from downslope than does the curve at location 2. This is because topographic β is smaller at location 4. In fact, the region near location 2 is characterized by both the largest northward orientation of the isobaths and the largest topographic β (Fig. 9c). Both of these contribute to the greater eastward penetration of the dispersion curve there.

In the dispersion relations of Fig. 9b the zonal wavenumber of the 40-day Gulf Stream meanders is indicated by the heavy dashed line. The point at which the dispersion curve intersects this line denotes the (k, l) of the topographic wave that would couple to the meanders. Note that coupling is possible at sites 1, 2, and 4. However, because of the greater eastward penetration of the dispersion curve at site 2, the matching wavevector there is significantly smaller than at the other sites (i.e., the total wavelength is larger, as documented by the values of the matching λ listed in Fig. 9b). To show that the waves observed at the Inlet array do in fact originate near site 2, the model was used to trace the matching wave forward in time from location 2 and from location 4 (location 4 has the second largest matching wavelength; Fig. 9b). The ray paths of the two waves are shown in Fig. 10. Because of the smaller (total) wavelength at site 4, the group velocity is substantially reduced and the wave takes ten times longer to reach the Inlet array than does the wave originating from site 2 (Fig. 10). The trapping scale is also much smaller. By the time the wave from site 4 reaches the Inlet array, it has a wavelength of only 35 km and trapping scale of 450 m, clearly not observed in the Inlet data. The slow speed and small trapping scale imply that this wave would be more subject to frictional damping, hence it might decay before reaching the Inlet site. Furthermore, a group speed of only 7 km day^{-1} is less than the mean deep velocity in the Gulf Stream (Halkin et al. 1985), so in fact the wave might not be able to propagate against the Gulf Stream. The situation is similar for a wave traced from site 1 (not shown).

By contrast, the character of the wave originating from site 2 is basically the same as that traced backwards in Fig. 8, and hence agrees with the observed wave characteristics at the Inlet array. Thus, the region near 71°–72°W (shaded in Fig. 9a) does, in fact, appear to be the generation site of the observed 40-day topographic waves. It is the combination of large northward orientation of the isobaths and strong bottom slope at this location (shaded region in Fig. 9c) that leads to this coupling.

b. Meander bursts

It is likely that analogous coupling of eastward propagating meanders to topographic waves will occur at a variety of time and space scales. However, since 40-day meanders are most prevalent in the Gulf Stream it is this signal that dominates the observed deep variability, at least at the Inlet site. To investigate the long-

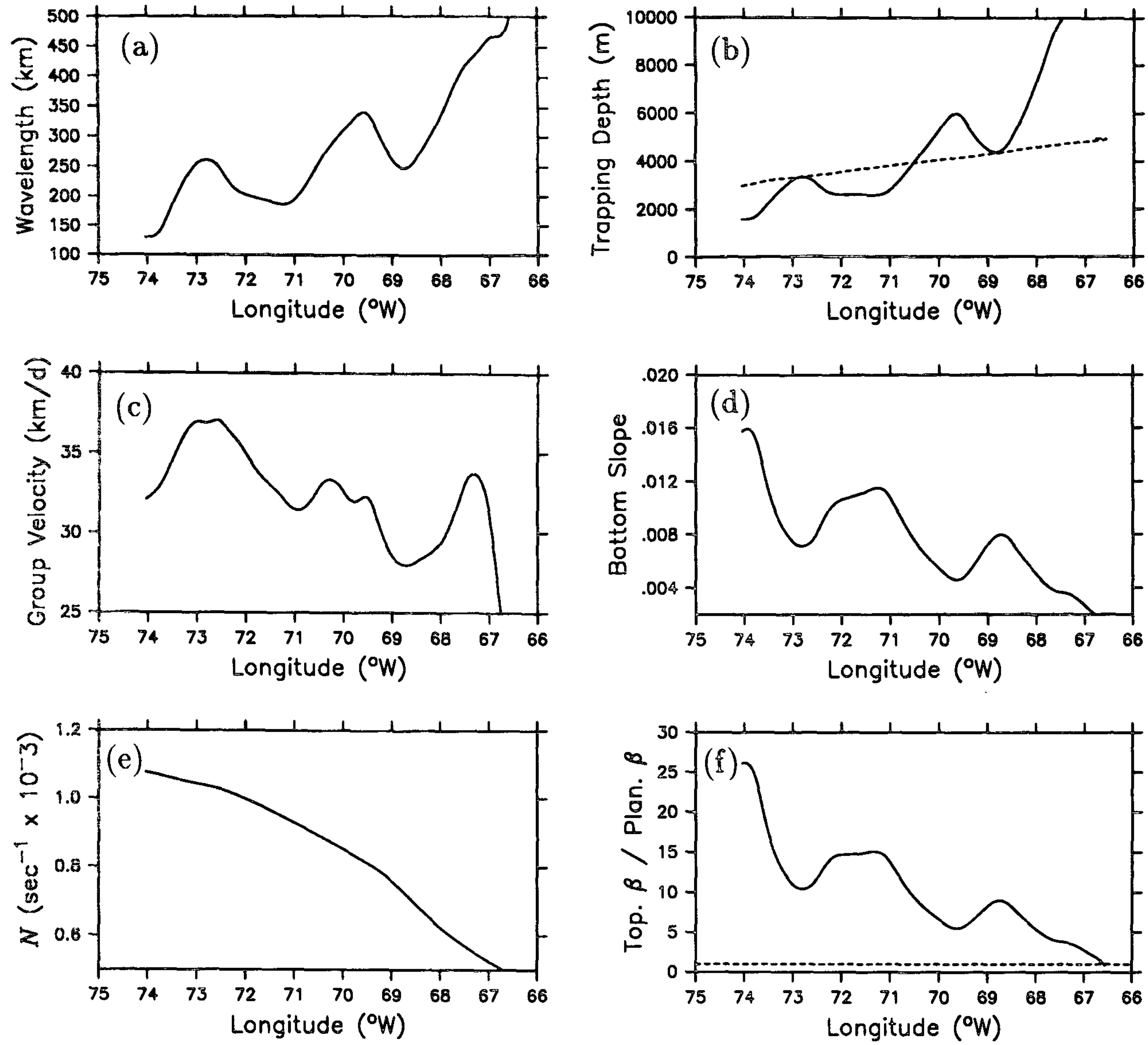

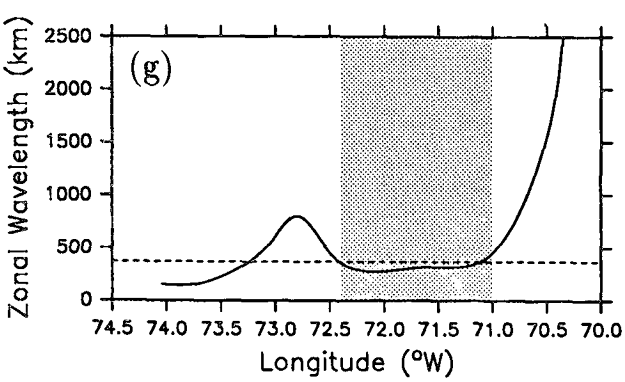

FIG. 8. Features of the 40-day Rossby wave along the ray path denoted by the asterisk in Fig. 7 (note: choosing any of the rays in Fig. 7 gives comparable results): (a) wavelength $2\pi/|\mathbf{k}|$; (b) vertical trapping scale $1/\lambda_v$ (solid line), bottom depth (dashed line); (c) group velocity; (d) bottom slope; (e) Brunt–Väisälä frequency N; (f) ratio of topographic β to planetary β (solid line), the dashed line is the value 1; and (g) zonal wavelength $2\pi/k$ (solid line). The dashed line is the wavelength of the most frequently occurring meander in the Gulf Stream. The shaded band marks the region over which the two curves match.

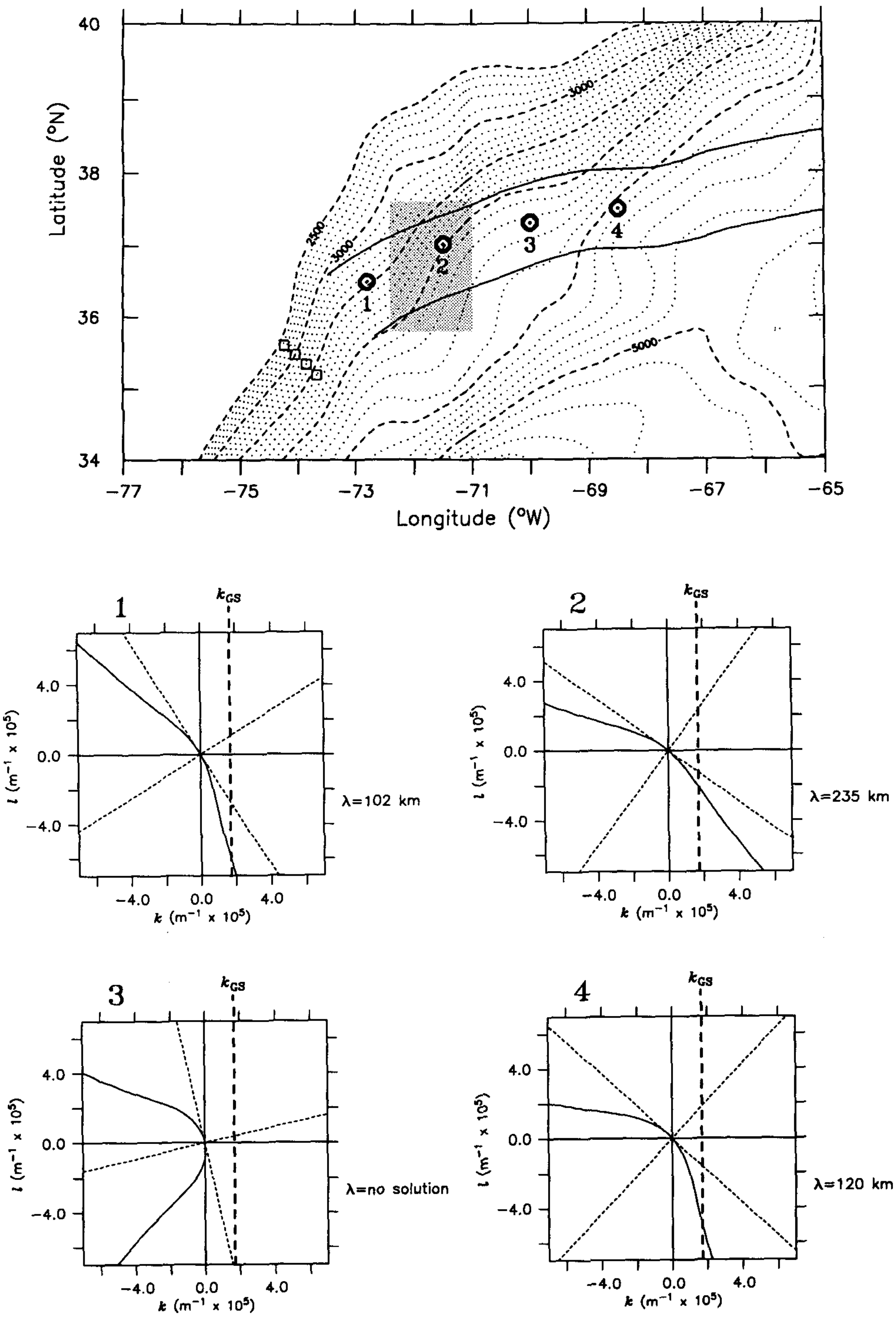

FIG. 9. (a) Locations along the axis of the deep Gulf Stream at which the dispersion curve was calculated (numbered circles). The shaded band is the region where the 40-day Rossby waves match the Gulf Stream meanders, according to Fig. 8g. (b) Rossby wave dispersion curve (heavy solid line) at the four locations in (a). The lightly dashed lines indicate the alongslope and cross-slope directions. The heavy dashed line denotes the zonal wavenumber k_{GS} of the most frequently occurring meander in the Gulf Stream. The total wavelength of the Rossby wave that matches k_{GS} is indicated to the right of each curve.

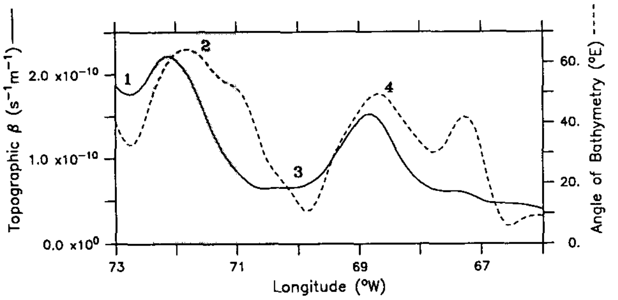

FIG. 9. (*Continued*) (c) Topographic β (solid line) and the angle of the bathymetry (dashed line) along the axis of the deep Gulf Stream. The four locations where the dispersion curve was calculated are marked. The shaded band marks the region of coupling as in (a).

term behavior of the 40-day Gulf Stream meanders, a complex demodulation was done on the lateral displacement time series of the Gulf Stream at the Inlet site (from the IES data). This calculation results in a time series of the amplitude of the 40-day meanders (Fig. 11b). Interestingly, the amplitude variation consists of a set of four bursts, comparable to the bursts of the observed deep waves (Fig. 11c) only offset in time: a burst in Gulf Stream meandering leads a topographic wave burst by ~80 days. The correlation of the two time series contains a peak at a lag of 80 days, significant at the 99% confidence level.

This offset is presumably the time it takes meanders to reach the generation site plus the time for the waves to propagate back to the Inlet site. However, the propagation speed of the meanders together with the group velocity of the waves (from the model) indicates that the elapsed time for this to occur is only 40 days. This discrepancy might be due to an advective offset to the wave group speed due to the eastward flowing Gulf Stream. To demonstrate this, a deep Gulf Stream velocity profile was computed by cross-stream averaging the core of a representative absolute velocity section at 73°W from Halkin et al. (1985). Next, the trapping scale of the wave versus distance along the ray was obtained from the model. Finally, the time for the wave to reach the Inlet site was computed using the net speed obtained by subtracting the mean Gulf Stream speed over the trapping scale from the group speed of the wave. This resulted in a total elapsed time of 75 days, in good agreement to the observed lag in Fig. 11.

The growth of 40-day meanders in the Gulf Stream, resulting in the observed bursts, implies that the Gulf Stream is particularly unstable to such waves. Johns (1988) developed a 1D baroclinic instability model using a realistic Gulf Stream potential vorticity profile near Cape Hatteras and found that the dominant unstable mode had a wavelength of 390 km and period of 28 days, intriguingly similar to the observed meanders. The observations of Rossby (1987) reveal that the mean to eddy energy conversion in this region of the Gulf Stream is, in fact, predominantly baroclinic, supporting Johns' (1988) approach. The Inlet array data suggest that the 40-day meander bursts might be associated with long timescale shifts in the location of the Gulf Stream. In particular, the bursts occur during the transition periods as the Gulf Stream moves either onshore or offshore (Fig. 11a). This might explain the alternating character of the deep wave signal discussed earlier (Fig. 4). Specifically, when a meander burst occurs as the Gulf Stream moves onshore, the subsequent wave burst is felt only at the base of the slope, whereas when the Gulf Stream moves offshore the wave burst is felt farther upslope. This might seem opposite of what is expected. However, when the Gulf Stream moves onshore the associated topographic wave ray spends most of the time in shallow water (Fig. 7) subject to increased dissipation; hence, the onshoremost portion of the wave might simply get damped out by the time it reaches the Inlet site. By contrast, when a ray approaches from deeper water, the friction does not have as long to act. This argument is of course qualitative and requires further testing.

In Johns' (1988) baroclinic instability model, the horizontal shear of the Gulf Stream was neglected, resulting in the following expression for the meridional gradient of potential vorticity:

$$Q_y \sim \beta - \frac{f_0^2}{N^2} u_{zz}, \tag{9}$$

where u is the zonal velocity of the Gulf Stream. Johns (1988) found that the change in sign of u_{zz} between 300 and 1500 m resulted in the dominant unstable mode. This change in sign is due to the increased cross-stream slope of the central thermocline of the Gulf Stream (say 12°C) versus that of the upper and lower thermocline (Fig. 12). This suggests that more strongly sloped isotherms in the central thermocline would result in conditions more favorable to baroclinic instability.

Since the IESs are sensitive only to variations in the central thermocline—here they are used to measure the depth of the 12°C isotherm (Z12)—the Inlet IES data can be used to consider the instability condition. The time series of Z12 along the middle line of the Inlet array (Fig. 1) were used to generate daily cross-stream profiles of the Gulf Stream Z12 interface. This was done using a spline fit to the values at the five instrument sites, following Pickart and Watts (1993). The average slope across the Gulf Stream front was then computed. No obvious relation was found between variations in frontal slope and the timing of the 40-day meander bursts. It is worth mentioning that the frontal slope calculation is quite noisy and should really be done using an array with finer cross-stream spacing (no such array has ever been deployed in the Gulf Stream). For this reason, the lack of a relationship between the instability condition and the meander bursts should not be considered as conclusive.

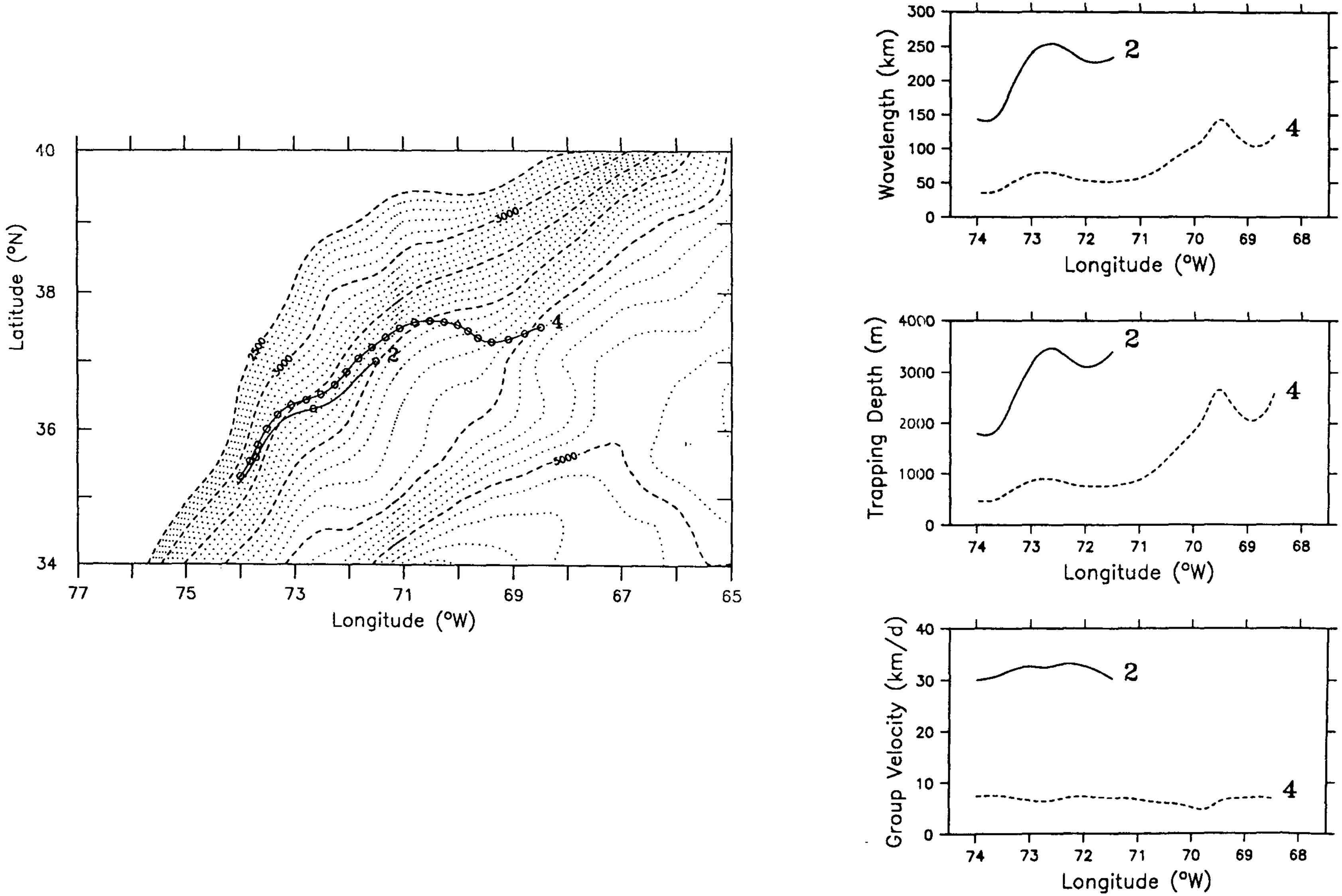

FIG. 10. Comparison of two 40-day Rossby waves matched to the most frequently occurring Gulf Stream meander at two different locations (sites 2 and 4 in Fig. 9a). (a) Forward-traced ray paths from the two locations. The circles denote 4-day intervals. (b) Comparison of total wavelength, trapping scale, and group velocity.

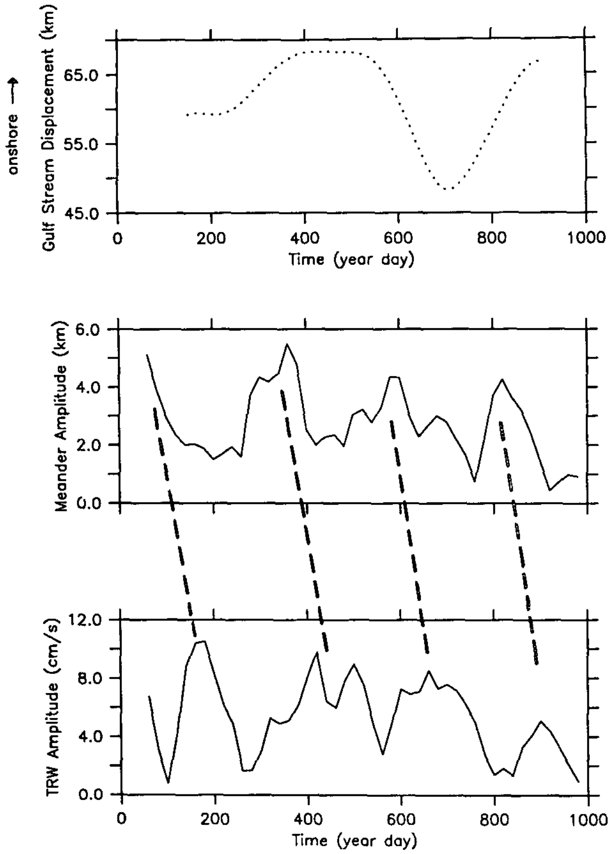

FIG. 11. (a) The 300-day low-passed lateral position of the Gulf Stream measured by where the depth of the 12°C isotherm = 400 m from the central line of IESs (Fig. 1). Increased displacement corresponds to more onshore. Year day 1 is 14 October 1987. (b) Amplitude of the 40-day Gulf Stream signal of lateral displacement at the central line from complex demodulation. (c) The 40-day topographic Rossby wave amplitude at BCM5 from Fig. 4, which lags the 40-day Gulf Stream meander signal by 80 days as indicated by the dashed lines.

The precise nature of the 40-day meander bursts, including the apparent regularity, thus remains an open question. The 40-day amplitude modulation of the Gulf Stream SST front over the longer 8-yr period (not shown) reveals that the bursts are persistent, with an average period of 280 days. Using the IES data, it can be shown that the long timescale shifts in Gulf Stream position coincident with the bursts are not simply the manifestation of slowly propagating large-scale meanders (see Pickart 1994). Lee (1994) finds that at periods longer than a year there is a domainwide latitudinal fluctuation of the Gulf Stream path, which may be related to this. Variation in the wind stress curl line should also be considered. Other factors that may influence the Gulf Stream and hence trigger the regularly occurring instability are variations in the DWBC fluctuations or the arrival of the wave bursts back at the Inlet site. This latter effect would mean that a complex feedback mechanism exists. Another possibility is that the length of the wave burst represents the natural life cycle of the instability. Clearly, more work is required to investigate these ideas.

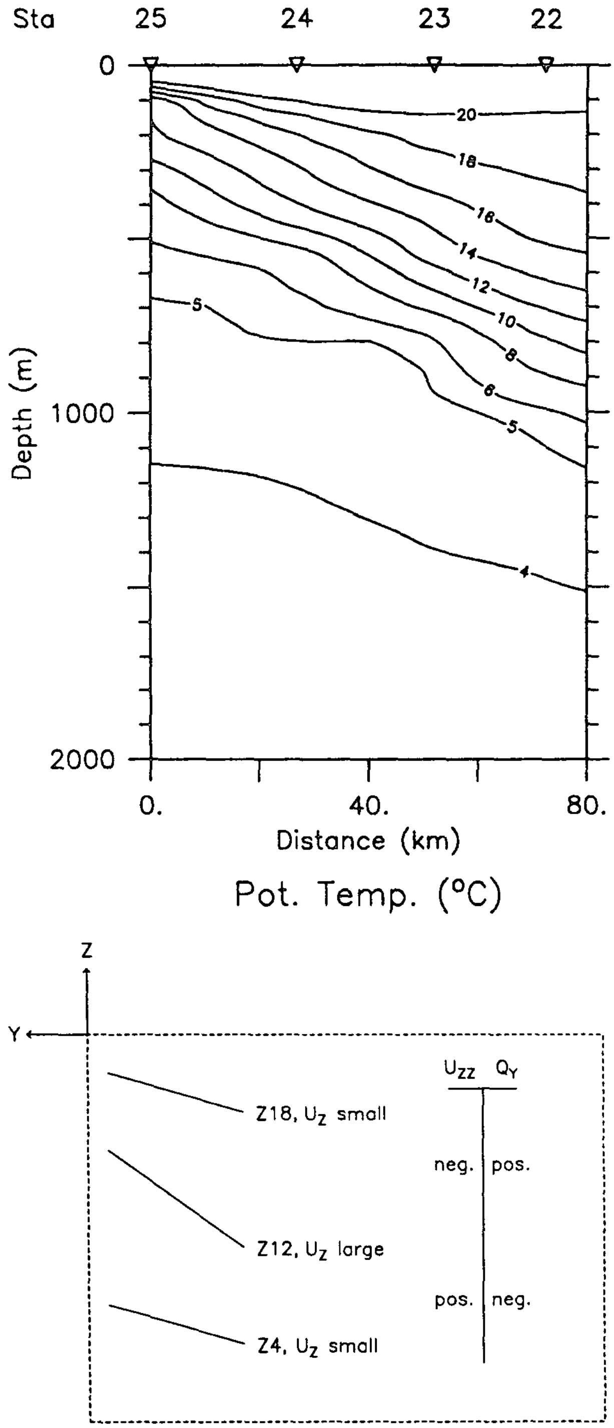

FIG. 12. (a) Temperature section across the Gulf Stream (from Pickart et al. 1992b). (b) Schematic illustrating the increased isotherm slope of the central thermocline in (a) and its implications (by thermal wind) on the meridional gradient of potential vorticity Q.

5. Summary

An analysis of three year's worth of bottom current meter records indicate that 40-day topographic Rossby waves occur in regular bursts along the continental slope off of Cape Hatteras. Using a ray tracing model, it was revealed that the waves are generated by associated bursts of eastward propagating 40-day meanders of the Gulf Stream. As the meanders pass a northward bend in the bathymetry near 71°–72°W, they are able to couple to topographic waves, which have eastward phase speed and a zonal wavelength that matches that of the meanders. The westward group speed of the waves brings them onshore, and they subsequently refract toward Cape Hatteras. These observations provide evidence that the Gulf Stream energy radiation mechanism described by Rizzoli et al. (1994) is at work in the ocean.

The 40-day Gulf Stream meanders are the most frequently occurring type of meander found in the Mid-Atlantic Bight, presumably because they represent the most dominant baroclinically unstable mode of the current in this region. Bursts of these meanders occur regularly with an average period of about 9 months and are associated with large-scale transitions in the position of the Gulf Stream. It still remains unclear what triggers the bursts and what determines their period.

Acknowledgments. I wish to thank Erik Fields who initiated the model development and Randy Watts and Chris Meinen who contributed to the refinements. Karen Tracey kindly provided the IES Gulf Stream time series. I also thank Nelson Hogg and Tony Lee for valuable discussions, the latter whom also provided unpublished Gulf Stream SST data. This work was supported under ONR Contracts N00014-92-J-1910, N00014-87K-0235, and N00014-92J-4013.

REFERENCES

Bower, A. S., and N. G. Hogg, 1992: Evidence for barotropic wave radiation from the Gulf Stream. *J. Phys. Oceanogr.*, **22,** 42–61.
Halkin, D., T. A. Rago, and T. Rossby, 1985: Data report of the Pegasus program at 73°W. Technical Report No. 85-2, University of Rhode Island, 198 pp.
Hogg, N. G., 1981: Topographic waves along 70°W on the continental rise. *J. Mar. Res.*, **39,** 627–649.
——, 1988: Stochastic wave radiation by the Gulf Stream. *J. Phys. Oceanogr.*, **18,** 1687–1701.
Johns, W. E., 1988: One-dimensional baroclinically unstable waves on the Gulf Stream potential vorticity gradient near Cape Hatteras. *Dyn. Atmos. Oceans,* **11,** 323–350.
——, and D. R. Watts, 1986: Time scales and structure of topographic Rossby waves and meanders in the deep Gulf Stream. *J. Mar. Res.*, **44,** 267–290.
——, T. J. Shay, J. M. Bane Jr., and D. R. Watts, 1994: Gulf Stream structure, transport, and recirculation near 68°W. *J. Phys. Oceanogr.*, submitted.
Leblond, P. H., and L. A. Mysak, 1978: *Waves in the Ocean.* Elsevier.
Lee, T., 1994: Variability of the Gulf Stream path observed from satellite infrared images. Ph.D. thesis, Graduate School of Oceanography, University of Rhode Island.
Louis, J. P., and P. C. Smith, 1982: The development of the barotropic radiation field of an eddy over a slope. *J. Phys. Oceanogr.*, **12,** 56–73.
——, B. D. Petrie, and P. C. Smith, 1982: Observations of topographic Rossby waves on the continental margin off Nova Scotia. *J. Phys. Oceanogr.*, **12,** 47–55.
Meinen, C., E. Fields, R. S. Pickart, and D. R. Watts, 1993: Ray tracing on topographic Rossby waves. Graduate School of Oceanography Technical Report 93-1, University of Rhode Island, 43 pp.
Olson, D. B., O. B. Brown, and S. R. Emmerson, 1983: Gulf Stream frontal statistics from Florida Straits to Cape Hatteras derived from satellite and historical data. *J. Geophys. Res.*, **88,** 4569–4577.
Pedlosky, J., 1977: On the radiation of meso-scale energy in the mid-ocean. *Deep-Sea Res.*, **24,** 591–600.
Pickart, R. S., 1994: Interaction of the Gulf Stream and deep western boundary current where they cross. *J. Geophys. Res.*, **99,** 22 155–22 164.
——, and D. R. Watts, 1990: Deep western boundary current variability at Cape Hatteras. *J. Mar. Res.*, **48,** 765–791.
——, and ——, 1993: Gulf Stream meanders over steep topography. *J. Geophys. Res.*, **98,** 6895–6905.
——, X. Qian, and D. R. Watts, 1992a: The SYNOP Inlet Experiment: Bottom current meter data report for October 1987 to August 1990 mooring period. Technical Report 91-1, Graduate School of Oceanography, University of Rhode Island, 39 pp.
——, T. K. McKee, and W. S. Smethie, Jr., 1992b: Hydrographic data from *ENDEAVOR* 214: A study of the Gulf Stream-deep western boundary current crossover. WHOI Technical Report 92-23. Woods Hole Oceanographic Institution, 108 pp.
Rizzoli, P. M., N. G. Hogg, and R. E. Young, 1994: Stochastic wave radiation by the Gulf Stream: Numerical experiments. *J. Phys. Oceanogr.*, submitted.
Rosenfeld, L. K., 1987: Tidal band current variability over the northern California Continental Shelf. Ph.D. thesis, Woods Hole Oceanographic Institution/Massachusetts Institute of Technology Joint Program in Oceanography and Oceanographic Engineering, WHOI-87-11, 237 pp.
Rossby, T., 1987: On the energetics of the Gulf Stream at 73W. *J. Mar. Res.*, **45,** 59–82.
Schultz, J. R., 1987: Structure and propagation of topographic Rossby waves northeast of Cape Hatteras. M.S. thesis, Marine Sciences Program, University of North Carolina, 63 pp.
Thompson, R. O. R. Y., and J. R. Luyten, 1976: Evidence for bottom-trapped topographic Rossby waves from single moorings. *Deep-Sea Res.*, **23,** 629–635.
Welsh, E. B., N. G. Hogg, and R. M. Hendry, 1991: The relationship of low frequency deep variability near the Hebble site to Gulf Stream fluctuations. *Mar. Geol.*, **99,** 303–317.